

# Impact of hydromechanical stress on CHO cells' metabolism and productivity: Insights from shake flask cultivations with online monitoring of the respiration activity

Anne Neuss, Jacinta Sofia Tomas Borges, Nele von Vegesack, Jochen Büchs, Jørgen Barsett Magnus\*

Biochemical Engineering (AVT.BioVT), RWTH Aachen University, Aachen, Germany

## ARTICLE INFO

### Keywords:

CHO  
Hydromechanical stress  
Energy dissipation rate  
Oxygen transfer rate  
Power input  
Shake flask

## ABSTRACT

The hydromechanical stress is a relevant parameter for mammalian cell cultivations, especially regarding scale-up processes. It describes the mechanical forces exerted on cells in a bioreactor. The maximum local energy dissipation rate is a suitable parameter to characterize hydromechanical stress. In literature, different studies deal with the effects of hydromechanical stress on CHO cells in stirred tank reactors. However, they often focus on lethal effects. Furthermore, systematic examinations in smaller scales like shake flasks are missing. Thus, this study systematically considers the influence of hydromechanical stress on CHO DP12 cells in shake flask cultivations. By utilizing online monitoring of the oxygen transfer rate, the study simplifies and enhances the resolution of examinations. Results indicate that while lethal effects are absent, numerous sub-lethal effects emerge with increasing hydromechanical stress: The process time is prolonged. The time of glucose and glutamine depletion, and the lactate switch correlate positively linear with the logarithmic average energy dissipation rate while the maximum specific growth rate correlates negatively. Strikingly, the final antibody concentration only declines at the highest tested average energy dissipation rate of  $3.84 \text{ W kg}^{-1}$  (only tested condition with a turbulent flow regime and therefore a higher maximal local energy dissipation rate) from about  $250 \text{ mg L}^{-1}$  to about  $180 \text{ mg L}^{-1}$ . This study presents a straightforward method to examine the impact of hydromechanical stress in shake flasks, easily applicable to any other suspension cell line. Additionally, it offers valuable insights for scale-up processes, for example into stirred tank reactors.

## 1. Introduction

Nowadays, the cultivation of Chinese hamster ovary (CHO) cells in suspension cultures is well-established for the production of biopharmaceuticals [1]. In industry, stirred tank reactors (STRs) are the common choice for antibody production with titers of  $3\text{--}8 \text{ g L}^{-1}$  at production scale [2]. The most important safety aspect is to keep the product quality constant [3]. To achieve this objective, it is crucial to control process parameters and stay in a defined operating range [4]. Because process development and evaluation are often performed in smaller scales, the process parameters have to be kept constant over scales. Thus, scale-independent parameters like  $\text{O}_2$  transfer,  $\text{CO}_2$  removal, temperature, or the maximum hydromechanical stress are

particularly suitable for the characterization of a process [5]. Nevertheless, many current processes are based rather on historical and empirical evidence than on a fundamental understanding of those important parameters [6,7]. Already at the beginning of adapting mammalian cells to suspension in the 1980s, it was evident that forces by stirring or shaking are a decisive parameter [8]. Due to the lack of a cell wall and the comparably big size of mammalian cells, they were considered as extremely sensitive to stirring or shaking [6,9]. Consequently, some early studies on the influence of stirring on animal cells were conducted, analyzing under which condition cell damage occurs [10–12]. Nowadays, large-scale systems are still stirred with low agitation rates resulting in insufficient mixing and gradients of nutrients and byproducts [13]. Chalmers, therefore, even stated that not the

*Abbreviations:* P/V, volumetric power input;  $\epsilon$ , energy dissipation rate; Re, Reynolds number;  $\mu$ , specific growth rate; OTR, oxygen transfer rate; OUR, oxygen uptake rate; TOM, Transfer-rate Online Measurement device; Ne', modified Newton number for shake flasks.

\* Corresponding author.

E-mail address: [Jorgen.Magnus@avt.rwth-aachen.de](mailto:Jorgen.Magnus@avt.rwth-aachen.de) (J.B. Magnus).

<https://doi.org/10.1016/j.nbt.2024.09.008>

Received 13 June 2024; Received in revised form 20 September 2024; Accepted 28 September 2024

Available online 5 October 2024

1871-6784/© 2024 The Authors. Published by Elsevier B.V. This is an open access article under the CC BY license (<http://creativecommons.org/licenses/by/4.0/>).

hydromechanical forces in the bioreactor are responsible for certain effects but the insufficient mixing resulting from the low stirring intensities [6]. Thus, the issue arises as to whether cells would be able to withstand higher hydromechanical forces. In order to approach this question, it will first be considered how hydromechanical stress can be quantified, which variables describe it correctly, and how it can be measured.

Hydromechanical stress arises due to the movement or flow of fluids and comprises different types of stresses [8,14]. This is present in stirred or shaken bioreactors, but also in hoses or downstream devices [8]. The hydromechanical stress is affected by mixing, aeration (especially bubble forming and bursting), and laminar or turbulent flows within a liquid [15,16]. As hydromechanical stress cannot be measured directly, parameters must be found to quantify it. In literature, the following parameters have become established: (1) the volumetric power input (P/V) (2) the energy dissipation rate ( $\epsilon$ ), and (3) the Kolmogorov's length of microscale ( $\lambda_K$ ) [17]. The latter describes the cascade process of forming smaller eddies out of large-scale turbulent eddies [18]. According to the theory, cell damage occurs if the size of the eddies is smaller or similar to the size of the cells [19]. After this theory, animal cells should not be sensitive to hydromechanical stress when keeping the eddy sizes above roughly 18–20  $\mu\text{m}$  (upper size of CHO cells) [20]. A more quantitative concept is the consideration of  $\epsilon$  [ $\text{W kg}^{-1}$ ] or the corresponding P/V [ $\text{W m}^{-3}$ ]. P/V describes the power input per liquid volume into the reactor.  $\epsilon$  describes the irreversible conversion of kinetic energy to heat and is calculated by dividing P/V by the liquid density ( $\rho$ ) [15]. It is well known that  $\epsilon$  values strongly depend on its spatial distribution in bioreactors [7]. Therefore, the maximal  $\epsilon$  ( $\epsilon_{\text{max}}$ ) or the quotient of  $\epsilon_{\text{max}}$  to the average  $\epsilon$  ( $\epsilon_{\theta}$ ) is considered to be a suitable term for quantifying hydromechanical stress [14,21]. Up to date, several different methods to determine  $\epsilon_{\text{max}}$  have been established: indirect measurements using shear-sensitive systems like the maximum stable drop size [14,22], flocculation systems [21,23], or shear-sensitive layer aggregates [24] and direct methods like Laser-Doppler anemometry, particle image velocimetry or constant temperature anemometry [24]. For studying the effect of different  $\epsilon$  on mammalian cells, different methods and devices concerning different phases (from upstream to downstream) of cultivation were developed and reviewed in detail elsewhere [6,8]. Chalmers and coworkers for example developed a microfluidic device where they pumped cells through capillaries mimicking different  $\epsilon$  [25]. In the first studies, where the cells were exposed to hydromechanical stress only once, cell damage occurred only at an  $\epsilon$  of  $100 \text{ W kg}^{-1}$  [25,26]. Later on, the authors analyzed exposure to repeated hydromechanical stress to CHO cells and reported lethal effects from  $6.4 \times 10^3 \text{ W kg}^{-1}$  and sub-lethal effects from  $60 \text{ W kg}^{-1}$  [27,28]. However, they used hydromechanical stress only in a laminar regime in capillaries and achieved very high tolerable values [20]. Nienow and colleagues [20] found that cells in an aerated STR with  $\epsilon_{\theta} = 25 \text{ W kg}^{-1}$  can grow to the same cell density as in their standard operation conditions of  $\epsilon_{\theta} = 0.01\text{--}0.02 \text{ W kg}^{-1}$ . Siek et al. [15] used a 2 L bioreactor as a scale-down model that mimicked the hydromechanical stress of large-scale bioreactors. The study included aeration, agitation, and laminar and turbulent flows. They observed different sub-lethal effects: In comparison to their standard  $\epsilon_{\theta}$  of  $0.01 \text{ W kg}^{-1}$ , the productivity decreased by 25 % at an  $\epsilon_{\theta}$  of  $0.4 \text{ W kg}^{-1}$ . The decrease was even stronger when the cells were exposed to an  $\epsilon_{\theta}$  that was periodically oscillating between these two values. The authors did not detect any differences in metabolite consumption, byproduct formation, or product quality [15]. In a second study, they investigated the effect of sparging, aeration, and the combination of both individually and identified an influence on viability but not on metabolism, productivity, or product quality [16]. Neunstöcklin and coworkers [5] analyzed the influence of hydromechanical stress on CHO and Sp2/O cells (B lymphocyte cells) with a scale-down model consisting of an external loop at a bioreactor with nozzles of different diameters. Laminar and turbulent flows were tested in oscillatory manners. They observed thresholds of hydromechanical stress where below this value

the cells do not show any response. Above this threshold, CHO cells reacted with better growth but reduced productivity [5]. By transferring the method to a large-scale fermenter, the authors could show that the hydromechanical stress does not depend on the size of the reactor [29]. Up to now, most of the process engineering considerations concerning the hydromechanical stress of mammalian cells were conducted in STRs or scale-down devices mimicking them. Furthermore, only a few of these approaches dealt with the investigation of sub-lethal effects. However, the development of CHO production processes normally starts in smaller scales like shake flasks or microtiter plates. The first vessels in seed trains are normally also shake flasks [30]. Furthermore, efforts are being made to bring shaken systems to production scale [31].

The fundamentals of  $\epsilon$  and the hydromechanical stress in shake flasks were in detail investigated by Büchs and Zoels [32] and Peter et al. [22]. They established a correlation for determining  $\epsilon_{\theta}$  and  $\epsilon_{\text{max}}$  in shake flasks and revealed that the shaking diameter and the filling volume have no impact on the hydromechanical stress, whereas it is influenced by the flask size and the shaking frequency. They also found that the P/V needed for generating the same hydromechanical stress as in STRs is tenfold larger in shake flasks [22]. To our knowledge, only two approaches considered the hydromechanical stress on CHO cells in shake flasks in a detailed process engineering way up to now. Maschke et al. [17] defined design spaces using the concept of Kolmogorov's scale of turbulence where the probability of failure for a CHO cultivation is defined. They asserted that a P/V up to  $900 \text{ W m}^{-3}$  is suitable. However, they did not analyze sub-lethal effects [17]. Pérez-Rodriguez in contrast studied sub-lethal effects at two different shaking frequencies and shaking diameters. However, they used parameters leading to out-of-phase conditions and calculated  $\epsilon_{\text{max}}$  even though the criteria for using the corresponding equation of a Reynolds number ( $\text{Re}$ )  $> 60,000$  was not given [33]. Therefore, the results must be considered with caution and are not comparable to our and other studies. From our perspective, a fundamental investigation of the hydromechanical stress in shake flasks is therefore of interest.

The most common parameters in former hydromechanical stress research for CHO cells were the viable cell density (VCD) or the specific growth rate ( $\mu$ ) [5,7,15,17,34]. Both of these parameters are directly correlated to the oxygen uptake rate (OUR) [35–37]. The importance of the OUR as a key parameter was highlighted and reviewed recently [38] as well as the options to monitor it in small scales [39]. The OUR in low-breathing mammalian cell cultures is very close to the oxygen transfer rate (OTR) because the changes in the oxygen concentration in the liquid over time are negligible [35]. An appropriate way of monitoring the OTR in shake flasks for mammalian cells is the use of the Transfer-rate Online Measurement (TOM) system [35,36,40,41]. It determines the OTR non-invasively and online by using electrochemical sensors. Therefore, OTR monitoring is an easy way of analyzing the effect of different energy dissipation on CHO cell cultures.

The purpose of this study is to examine the impact of hydromechanical stress on CHO cells in shake flasks by varying the energy dissipation in a systematic process engineering manner. The impact on the cells' activity and metabolism is studied by monitoring the OTR. Furthermore, the impact on productivity will be analyzed.

## 2. Materials and methods

### 2.1. Cell line and culture medium

In this study, the suspension-adapted cell line CHO DP12 (clone#1934, ATCC CRL-12445) was utilized as a model production cell line. It produces an anti-IL-8 antibody.

The cells were cultivated in a chemically defined medium, TCX6D (Sartorius, Goettingen, Germany), supplemented with 8 mM glutamine (Sigma Aldrich/Merck, Darmstadt, Germany). During pre-cultures, 200 nM methotrexate (MTX, Sigma Aldrich/Merck) was added to the culture to prevent the transgene's loss. MTX was not supplemented to the main

culture experiments.

## 2.2. Cell cultivation

Cells were stored in the vapor phase of liquid nitrogen and thawed rapidly for all pre-cultures. The exact methods are described elsewhere [41].

All pre-culture cultivations were conducted at 36.5 °C and with a shaking frequency of 140 rpm at a shaking diameter of 50 mm. The pre-cultures were either performed in a Kuhner incubator (ISF1-X Kühner AG, Birsfelden, Switzerland) or on a Kuhner LSB-shaker (Kühner AG). The atmosphere in the ISF1-X incubator was regulated to 5 % CO<sub>2</sub> and a humidity of 70 %. The cells were cultured in 250 mL Corning polycarbonate Erlenmeyer flasks (Corning, Glendale, USA) with a vent-cap. On the Kuhner LSB-shaker, cells were cultivated in 250 mL glass TOM flasks (Kühner AG). Every glass flask was flushed with a gas mixture of 5 % CO<sub>2</sub> in synthetic air by an in-house built construction. All pre-cultures were passaged every 3–4 days to a cell density of approximately 3 × 10<sup>5</sup> cells mL<sup>-1</sup>. The shake flasks were filled with 20–50 mL of cell suspension.

The main cultures were all carried out in the Kuhner incubator ISF1-X. All cultivations were performed at 36.5 °C, 70 % humidity, and 5 % CO<sub>2</sub>. According to the experiment (see also Table 1), 100, 250, or 500 mL glass flasks were used. The 100 and 500 mL standard Erlenmeyer flasks (DWK LifeScience, Wertheim, Germany) were closed with flex caps (Kühner AG). The 250 mL flasks were TOM flasks (Kühner AG). The filling volume for all flasks was 20 % of the nominal flask volume. The shaking frequency was varied from 140 to 450 rpm, and the shaking diameter was set to 50 or 25 mm accordingly (see Table 1). All cultivations were started with an initial VCD of 5 × 10<sup>5</sup> cells mL<sup>-1</sup>.

## 2.3. Monitoring of the OTR

In all main culture experiments, the OTR was monitored by the Kuhner TOM device (Kühner AG). This is a slightly modified commercial version of the RAMOS (Respiration Activity Monitoring System) device [42,43]. The measuring principles are described elsewhere [42]. The measurement cycle was set to 60 min in total with a measuring phase of 18 min and a flow phase of 42 min. The calculation of the OTR is temperature-dependent. Consequently, outliers in the OTR occur after opening the incubator hood for sampling. Those outliers were removed from the data and excluded from graphs and further analysis.

## 2.4. Sampling

The main-culture experiments were sampled manually every day. Therefore, 1.5 mL of culture broth was taken from offline shake flasks daily. VCD and viability were determined directly after sampling (see determination of offline parameters). The remaining culture broth was centrifuged for 3 min at 2000 g (mini centrifuge Rotilabo, Carl Roth, Karlsruhe, Germany). The supernatant was stored at –20 °C until they were further analyzed.

## 2.5. Determination of offline parameters

### 2.5.1. VCD and viability

VCD and viability were measured with a CEDEX AS20 device (Roche, Basel, Switzerland). 300 µL of cell suspension were filled into cups and supplied to the device. The CEDEX uses the trypan blue exclusion method to determine VCD and viability. The device stains samples automatically with 1:2 diluted Trypan Blue Solution to distinguish living from dead cells (Gibco/Thermo Fisher Scientific, Waltham, USA).

### 2.5.2. Glucose and lactate concentrations

Glucose and lactate concentrations in the supernatant were determined by an HPLC method. An organic acid resin column (Rezex ROA Organic Acid H+ (8 %), 300 × 7.8 mm, Phenomenex Inc., Torrance, USA) was used for separation. The flow rate was set to 0.8 mL min<sup>-1</sup> and the temperature to 40 °C. 5 mM H<sub>2</sub>SO<sub>4</sub> was used as the mobile phase and the isocratic mode for separation. For detection, a refractive index detector (RefractoMax 520, Shodex, Munich, Germany) was utilized. The HPLC system was the Dionex Ultimate 3000 system (Thermo Scientific, USA).

### 2.5.3. Glutamine concentration

To determine the glutamine concentration in the supernatant, the kit L-Glutamine / Ammonia (Rapid) (Megazyme Ltd., Bray, Ireland) was used according to the manufacturer's instructions.

### 2.5.4. Antibody concentration

For determination of the IgG antibody concentration in the supernatant, a Chromolith® Protein A column (4.6 × 25 mm, Sigma Aldrich/Merck) with a pore size of 300 Å was used with an in-house protocol.

## 2.6. Calculation and correlations

### 2.6.1. Determination of P/V, ε, Re and λ<sub>K</sub> in shake flasks

The power input in shake flasks (Eq. 1) was calculated according to [44] including the modified Newton number for shake flasks (Ne'), the liquid density (ρ) [kg m<sup>-3</sup>], the shaking frequency (n) [s<sup>-1</sup>], the maximum inner flask diameter (d) [m] and the filling volume (V<sub>L</sub>) [m<sup>3</sup>].

$$\left(\frac{P}{V}\right)_{\phi} = Ne' \times \rho \times \frac{n^3 \times d^4}{V_L^{2/3}} \quad (1)$$

The corresponding ε<sub>φ</sub> is defined by Eq. (2) according to [45].

$$\varepsilon_{\phi} = \left(\frac{P}{V}\right)_{\phi} \times \frac{1}{\rho} = Ne' \times \frac{n^3 \times d^4}{V_L^{2/3}} \quad (2)$$

Re was calculated by using Eq. (3) with the dynamic viscosity of a fluid (η) [Pa • s].

$$Re = \rho \times \frac{n \times d^2}{\eta} \quad (3)$$

For Re > 60 000, ε<sub>max</sub> is calculated by Eq. (4) if the Froude number is > 0.4 and with the shaking diameter (d<sub>0</sub>) [45].

**Table 1**

Characteristic parameters of shake flask cultivations. ε<sub>φ</sub>, ε<sub>max</sub>, Re and λ<sub>K</sub> were calculated by using Eqs. (2–5).

Flask size [mL]	Filling volume [mL]	Shaking frequency [rpm]	Shaking diameter [mm]	ε <sub>φ</sub> [W kg <sup>-1</sup> ]	ε <sub>max</sub> [W kg <sup>-1</sup> ]	Re [-]	λ <sub>K</sub> [µm]
100	20	140	50	0.08	0.08	8400	59
250	50	140	50	0.12	0.12	15423	54
250	50	200	50	0.32	0.32	22032	42
250	50	350	50	1.45	1.45	38557	29
500	100	450	25	3.84	17.0	76508	15

$$\begin{aligned} \varepsilon_{\max} &= 0.1 (\pi \times n \times d)^3 / h_1 \text{ with } h_1 \\ &= 1.11 \times d_0^{0.18} \times d^{-0.11} \times n^{0.44} \times V_L^{0.34} \end{aligned} \quad (4)$$

$\lambda_K$  is calculated according to Kolmogorov by Eq. (5) with the kinematic viscosity  $\nu$  [ $\text{m}^2 \text{s}^{-1}$ ].

$$\lambda_K = \sqrt[4]{\frac{\nu^3}{\varepsilon_{\max}}} \quad (5)$$

### 2.6.2. Determination of $\mu_{\max}$

The calculation of  $\mu$  from the OTR is generally calculated by Stöckmann et al. [37] as shown in Eq. (6).

$$\mu = \frac{\ln(OTR_t) - \ln(OTR_{t_n})}{t - t_n} \quad (6)$$

All calculations in this study were performed in MATLAB® (Mathworks, Inc.). For calculation, the data of any individual experiment up to the OTR peak were used. The period for calculation was set to five measuring points (corresponding to 5 h). From all calculated values the maximal specific growth rate ( $\mu_{\max}$ ) was defined. Only data with an  $R^2$  (coefficient of determination) greater than 0.9 were considered. Afterward, the mean value of the replicates was calculated [46].

### 2.6.3. Determination of cell-specific production and uptake rates

The cell-specific production or uptakes rates ( $q$ ) of the metabolites lactate, glucose, glutamine and the antibody were calculated according to Eq. (7).

$$q = \frac{1}{\text{VCD}} \times \frac{d\text{metabolite or antibody}}{dt} \quad (7)$$

### 2.6.4. Correlations of metabolites, $\mu$ , and the antibody concentration with $\varepsilon_\emptyset$

The time of glutamine and glucose depletion were identified from the changes in the OTR as shown in Fig. 1. The glutamine depletion leads to a short halt in the increase in the OTR while the glucose depletion leads to a rapid fall in OTR. The times of depletion were read out by drawing a vertical straight line from the characteristic changes in the OTR to the x-axis. This method of using the OTR signal to identify depletions and limitations of nutrients has been demonstrated in several other applications before [47–49]. In this work, the same principle was used for CHO cells. The time of lactate depletion was determined accordingly by using the offline lactate data. The time differences of the depletions to the depletions in the standard cultivation ( $\varepsilon_\emptyset = 0.12 \text{ W kg}^{-1}$ ) was calculated for all time points.  $\mu_{\max}$  was calculated as described in Determination of  $\mu_{\max}$ . The time differences of glucose and glutamine depletion and the lactate switch as well as  $\mu_{\max}$  were plotted against the logarithm of  $\varepsilon_\emptyset$ . A linear fit was applied (see Figs. 3 and 4).

The antibody concentrations of the last three measurement points (three days) were averaged and plotted against the logarithm of  $\varepsilon_\emptyset$  (see Fig. 5).

## 3. Results and discussion

### 3.1. OTR monitoring of CHO DP12 standard shake flask cultivations

The standard cultivation conditions in our laboratory for CHO cells are 250 mL shake flasks with a filling volume of 50 mL, shaken at a frequency of 140 rpm and a shaking diameter of 50 mm. The results of such standard cultivation are depicted in Fig. 1. The cells were cultivated in TOM glass shake flasks and connected to the TOM device. Three replicates were cultivated for online monitoring of the OTR only and another three replicates were additionally sampled daily for offline analysis.

Fig. 1A displays the VCD and the viability of the CHO DP12 cultures. The VCD increases steadily over roughly 6 cultivation days to about

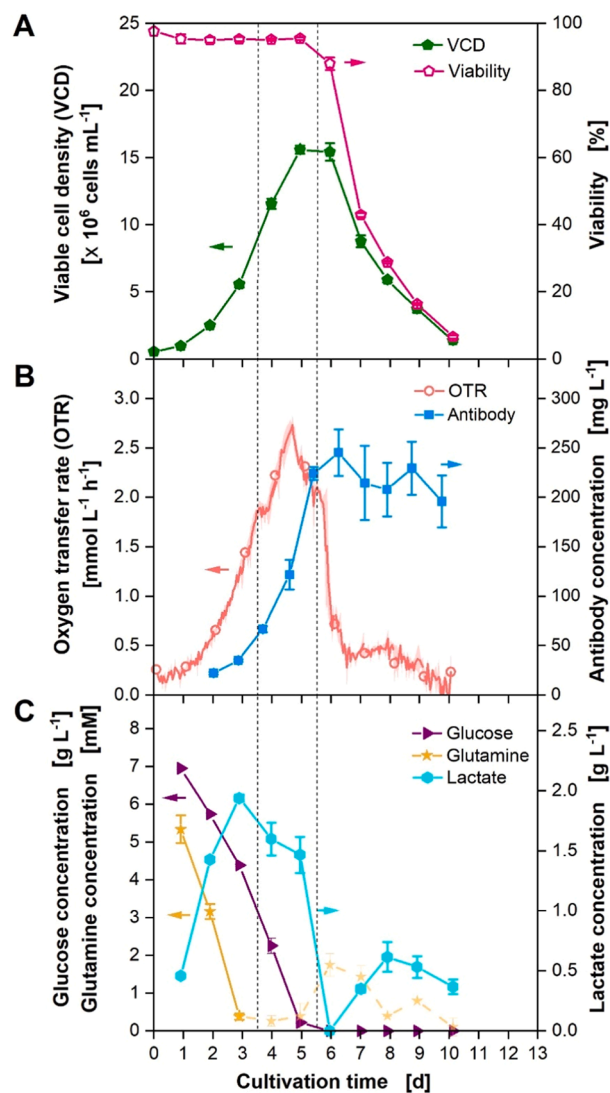


**Fig. 1.** Cultivation of CHO DP12 cells in shake flasks under standard conditions. The experiments were performed in six replicates. Three replicates were sampled daily for offline analysis and three were used for online monitoring only. All data are shown as mean value of three biological replicates (indicated as error bars or shades). A) Depicted are the viable cell density (VCD) and the viability determined by a CEDEX. B) Shown is the mean oxygen transfer rate (OTR). For clarity, only every 24th measuring point over time is marked as a symbol. The lines are drawn through all measured values. The outliers in the OTR data due to temperature adaptations after sampling were excluded from the data. In addition, the antibody concentration is shown. C) Corresponding glucose, glutamine, and lactate concentrations are plotted over time. Depletion of glucose and glutamine is marked by dotted vertical lines over all three parts of the figure. Cultivations were performed in a TOM device. Culture conditions: 250 mL TOM glass flasks, temperature ( $T$ ) = 36.5 °C, shaking frequency ( $n$ ) = 140 rpm, shaking diameter ( $d_0$ ) = 50 mm, filling volume ( $V_L$ ) = 50 mL, 5 %  $\text{CO}_2$ , 70 % rel. hum., medium: TCX6D + 8 mM glutamine; starting cell density:  $5 \times 10^5 \text{ cells mL}^{-1}$ .

$1.5 \times 10^7 \text{ cells mL}^{-1}$  (green line and closed pentagons) before it drops gradually until the end of cultivation on day 10. The viability (pink line and open pentagons) remains on a constant level above 96 % for 5 cultivation days before it decreases constantly. In Fig. 1B, the antibody concentration (blue line and closed squares) is shown. It rises until cultivation day 6 up to about 250  $\text{mg L}^{-1}$  and stays more or less on a constant level until the end of the cultivation. Hereby, literature-known values for the antibody titer are reached [50,51]. Fig. 1B additionally shows the OTR curve (red line and open circles) monitored in this



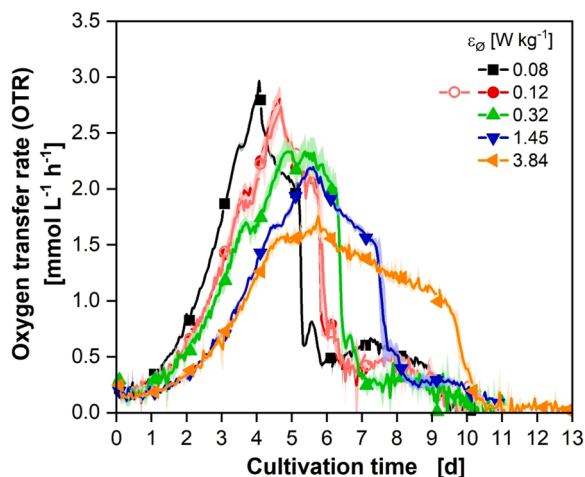


**Fig. 2.** Cultivation of CHO DP12 cells in shake flasks with varying average energy dissipation rates ( $\epsilon_0$ ). The mean oxygen transfer rate (OTR) of three replicates is shown with standard deviations illustrated as shaded areas. For clarity, only every twelfth measuring point over time is marked as a symbol. The lines are drawn through all measured data points. The outliers in the OTR data due to temperature adaptations after opening the incubation hood were excluded from the data. The curves in dark and light red are from the independent experiments depicted in Fig. 1 and Supp. Fig. S1. Culture conditions: flask size, shaking frequency, shaking diameter, and filling volume see Table 1, temperature (T) = 36.5 °C, 5 % CO<sub>2</sub>, 70 % rel. hum., medium: TCX6D + 8 mM glutamine; starting cell density:  $5 \times 10^5$  cells mL<sup>-1</sup>.

experiment by the TOM device. It rises to a maximum of about 2.8 mmol L<sup>-1</sup> h<sup>-1</sup>. The shape of the OTR curve resembles the shape of the VCD curve. The correlation of OTR and VCD was already shown by Ihling et al. for another CHO cell line [35,36]. The OTR is monitored with a 24-fold higher resolution of measuring points than the VCD (once per hour compared to once a day). This results in shoulders and kinks in the course of the OTR curve over time which are not visible in VCD and can be related to nutrient depletion. Regarding Fig. 1C, the relationship of those kinks and shoulders to offline parameters becomes apparent. The glucose concentration (purple line and triangles) decreases over the first 5 cultivation days. As soon as this carbon source is exhausted, the OTR curve drops sharply. The depletion of glutamine (ochre curve and stars) after about 3.5 days of cultivation is correlated to the shoulder in the OTR curve. The measurement method of glutamine by using a spectrophotometric kit is error-prone and subject to uncertainties. It is especially inaccurate at very low glutamine concentrations and when no glutamine is present anymore. This is the case for every measuring point after glutamine depletion. The CHO DP12 cell line exhibits a typical lactate switch which can be seen in Fig. 1C. Lactate increases until day 3 to about 2 g L<sup>-1</sup> before it is consumed again. The experiment was independently repeated (see Supp. Fig. S1) resulting in the same findings.

All in all, it could be demonstrated that OTR monitoring of the CHO DP12 cell line is feasible as an alternative to VCD determination providing a lot more information per time. Glutamine and glucose depletion are directly visible from the OTR curve.

### 3.2. Influence of varying $\epsilon_0$ on the OTR of CHO DP12 shake flask cultivations

To study the hydromechanical stress in shake flasks, the variation of P/V or the corresponding  $\epsilon_0$  was investigated as a suitable choice [22, 44]. As can be seen from Eqs. (1–2), P/V and  $\epsilon_0$  should be able to be varied by the nominal shake flask size (inner flask diameter), the shaking frequency, and the filling volume. However, Peter et al. showed the filling volume does not influence  $\epsilon_{max}$  and, thus, the

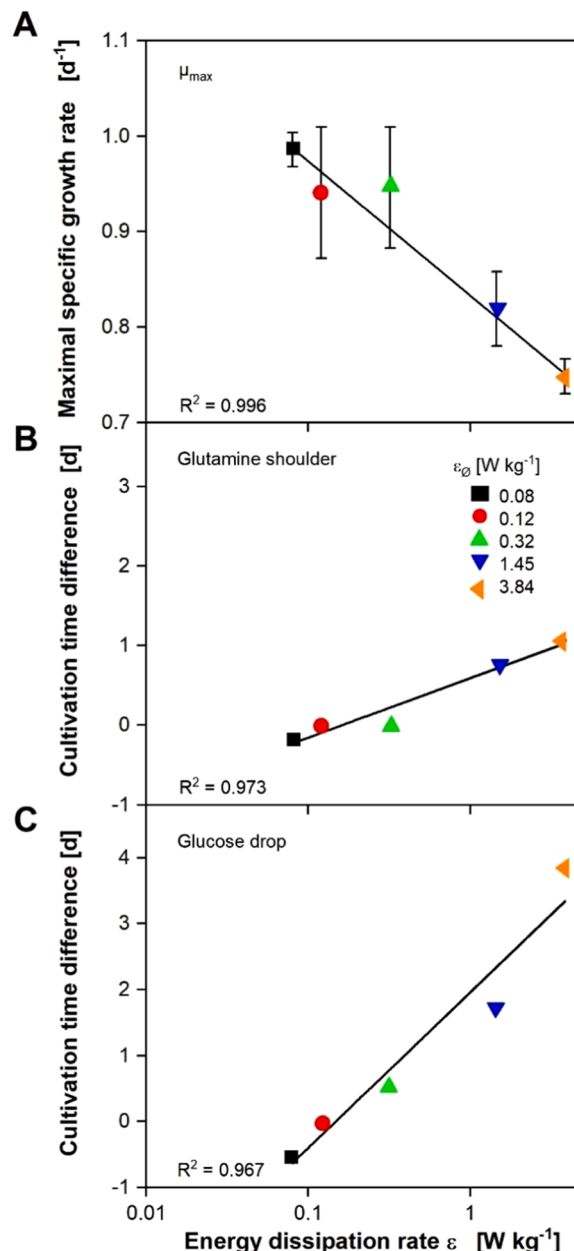


**Fig. 3.** Correlation of the maximal specific growth rate ( $\mu_{max}$ ) as well as the time of glucose and glutamine depletion to varying average energy dissipation rates ( $\epsilon_0$ ) for CHO DP12 cell cultivations.  $\epsilon_0$  is plotted logarithmically. A)  $\mu_{max}$  calculated from the individual replicates of the OTR data in Fig. 2. B) Cultivation time difference to the standard cultivation with  $\epsilon_0 = 0.12$  W kg<sup>-1</sup> of glutamine depletion read out from the glutamine shoulder in the OTR data in Fig. 2. C) Cultivation time difference to the standard cultivation with  $\epsilon_0 = 0.12$  W kg<sup>-1</sup> of glucose depletion read out from the glucose drop in the OTR data in Fig. 2. A linear fit was performed for all figures (shown as a black line).

hydromechanical stress [22]. Therefore, the relative filling volume was kept constant in the following experiments. The parameters used in this study and the corresponding calculated  $\epsilon_0$  and  $\epsilon_{max}$  are summarized in Table 1. The shaking diameter does not affect either parameter. However, it needed to be varied for the highest shaking frequencies because otherwise the liquid volume would overflow at the corresponding filling volume. In Table 1,  $\epsilon_0$  and  $\epsilon_{max}$  are listed. For shake flask experiments,  $\epsilon_{max}$  ( $P/V_{max}$ ) is equal to  $\epsilon_0$  ( $P/V_0$ ) if the Reynolds number is < 60,000 [22]. Furthermore,  $\lambda_K$  was calculated. As can be seen from Table 1,  $\lambda_K$  is larger than the maximal cell size of CHO cells (18–20  $\mu$ m) for  $\epsilon_0 \leq 1.45$  W kg<sup>-1</sup>. According to the theory of Kolmogorov, the cells should

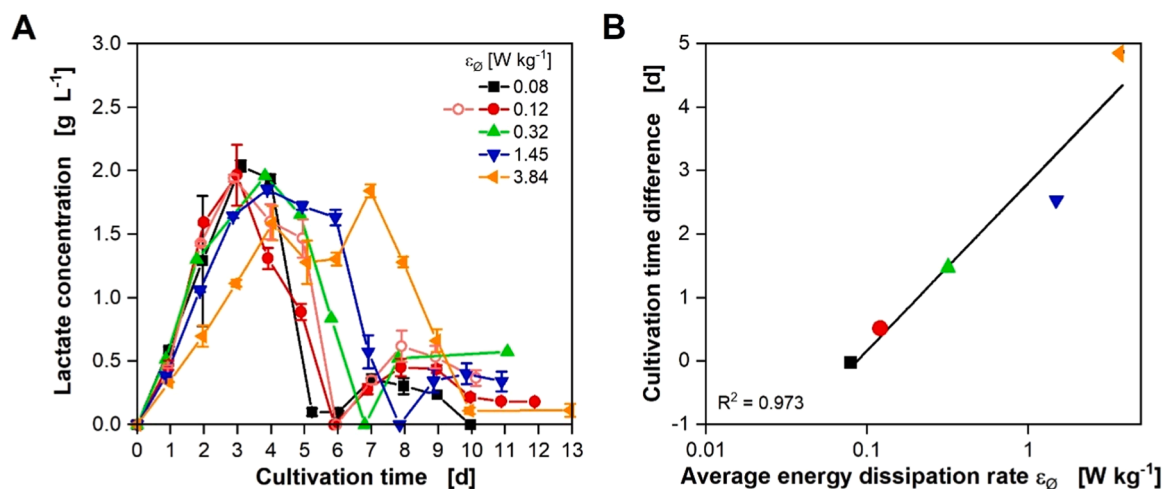


**Fig. 4.** Analysis of the lactate concentration of CHO DP12 cell cultivations in shake flasks at varying average energy dissipation rates ( $\epsilon_0$ ). A) Illustrated are the mean lactate concentrations of three biological replicates over time for the cultivations depicted in Fig. 2. B) The cultivation time difference to the standard cultivation with  $\epsilon_0 = 0.12 \text{ W kg}^{-1}$  of the lactate depletion read out from the offline data in A.  $\epsilon_0$  is plotted in logarithmic scale. Culture conditions: flask size, shaking frequency, shaking diameter, and filling volume see Table 1, temperature (T) = 36.5 °C, 5 % CO<sub>2</sub>, 70 % rel. hum., medium: TCX6D + 8 mM glutamine; starting cell density:  $5 \times 10^5 \text{ cells mL}^{-1}$ .

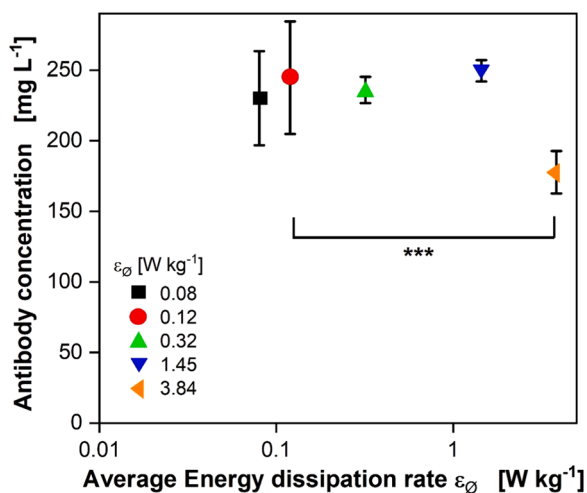


**Fig. 5.** Correlation of the final antibody concentration to the logarithm of varying average energy dissipation rates ( $\epsilon_0$ ) for CHO DP12 cell cultivations. The mean value of the last three cultivation days was calculated. Statistically significant differences against the reference cultivation ( $\epsilon_0 = 0.12 \text{ W kg}^{-1}$ ) are indicated by stars (\*\*\*) ( $p < 0.001$ ).

not be damaged for those cultivation conditions. For  $\epsilon_0 = 3.84 \text{ W kg}^{-1}$ ,  $\lambda_K$  is  $15 \mu\text{m}$  and therefore in the range of the cell's size. Based on Kolmogorov's theory, cell damage should occur in this range of energy dissipation.

Shake flask experiments for all  $\epsilon_0$  listed in Table 1 were conducted. Hence, a much wider range of different  $\epsilon_0$  was tested than in Maschke's work who tested up to roughly  $0.9 \text{ W kg}^{-1}$  [39]. The results of the OTR monitoring in this study are depicted in Fig. 2.

As becomes evident from Fig. 2, the shape of the OTR curves differentiate for varying  $\epsilon_0$  which corresponds to an altered respiratory activity. Thus, the sub-lethal effects of hydromechanical stress on CHO DP12 cells can be seen at first glance. For example, the maximum reached OTR value decreases with increasing  $\epsilon_0$  while the process duration is lengthened. It becomes also apparent that the increase of the OTR is slower with higher  $\epsilon_0$ . A detailed analysis of the metabolic differences is described in the following chapter (see Influence of varying  $\epsilon_0$  on the metabolism). The results are underpinned by VCD and viability

analysis (Supp. Fig. S2). Here, prolonged cultivation phases and lower maximal reached VCDs are visible with increasing  $\epsilon_0$ . Prolonged phases of high viability can also be observed. However, due to the higher data density of the online monitored OTR, the impact of the  $\epsilon_0$  on the cells behavior is much clearer from online monitoring and the online measured values are less error-prone and more independent from the operator than the offline analyses. Despite the altered shape of the OTR curves at varying  $\epsilon_0$ , all cultivations reached the same final oxygen transfer (integral of the OTR, see Supp. Fig. S3). It can be concluded that the cells consumed the nutrients completely in all cultivations independently of the hydromechanical forces present. This shows that – in contrast to what Maschke et al. found in their setup [17] – the CHO DP12 cells did not stop growing when reaching an  $\epsilon_0$  of about  $0.9 \text{ W kg}^{-1}$ . On the other hand, the results presented in this work are in accordance with the literature where lethal effects only occur at very high  $\epsilon_0$  [8,28,52]. In general, it must be mentioned that the different studies are hardly comparable with each other, as different cell lines, media, and setups were used. In this study, additional experiments were performed where the shaking frequency was only increased after two days of cultivation to vary  $\epsilon_0$  (Supp. Fig. S4). From these experiments, it can be concluded that the effect of different  $\epsilon_0$  is not due to lengthened lag phases, but to different levels of hydromechanical stress. Here, the OTR curves of  $\epsilon_0$  up to  $1.45 \text{ W kg}^{-1}$  are very close together. The OTR curves of  $\epsilon_0 = 2.88 \text{ W kg}^{-1}$  and  $\epsilon_0 = 3.84 \text{ W kg}^{-1}$  are noticeably different and show a lengthened cultivation time and a reduced maximal OTR similar to the experiments in Fig. 2.

### 3.3. Influence of varying $\epsilon_0$ on the metabolism

The impact of varying hydromechanical stress levels on the CHO DP12 cell line's metabolism will be further examined. For this, the OTR curves from Fig. 2 were analyzed concerning  $\mu_{\text{max}}$  and the two key metabolites glucose and glutamine whose consumption is directly visible from the OTR curve as described in the chapter OTR monitoring of CHO DP12 standard shake flask cultivations. The results are displayed in Fig. 3.

Fig. 3A shows the respective  $\mu_{\text{max}}$  for the different tested  $\epsilon_0$ .  $\mu_{\text{max}}$  was calculated as described in the chapter Determination of  $\mu_{\text{max}}$ . As it becomes evident,  $\mu_{\text{max}}$  decreases with an increasing  $\epsilon_0$  from roughly  $1 \text{ d}^{-1}$  (black square) for the lowest  $\epsilon_0$  to approximately  $0.75 \text{ d}^{-1}$  (orange left side triangle) for the highest  $\epsilon_0$ . From the visualization of the data, it is evident that  $\mu_{\text{max}}$  is in a good semi-logarithmic correlation ( $R^2 = 0.996$ )

with  $\varepsilon_0$  implying that higher hydromechanical stress makes the CHO DP12 cells as a whole grow slower. This can be due to two reasons: 1. every single cell is growing slower or 2. some cells do not survive because of hydromechanical stress. In literature, effects on  $\mu_{\max}$  were also associated with different impacts of hydromechanical stress. In contrast to this study, Neunstöcklin et al. observed better growth with increasing hydromechanical stress but overall only slight differences between different stresses [5]. In the setup of Maschke et al., who used 500 mL shake flasks, a reduced growth rate was observed at an  $\varepsilon_0$  of approximately  $0.9 \text{ W kg}^{-1}$  [17]. However, they did not test  $\varepsilon_0$  above this value.

The time of glutamine and glucose depletion were set in relation to this time of the standard cultivation with  $\varepsilon_0 = 0.12 \text{ W kg}^{-1}$  and plotted against the logarithm of  $\varepsilon_0$  (Fig. 3B). There is a logarithmic correlation of the time difference values for both metabolites with  $\varepsilon_0$ . With an increasing  $\varepsilon_0$ , glutamine and glucose are depleted later in the cultivation process which is a logical consequence of the reduced growth rate. Without the online OTR data, the effect would not have been obvious. The offline data (see Supp. Fig. S5) confirm the observations but because of the lower data density, the trend is less well visible. Additionally, the cell-specific glucose and glutamine uptake rates were calculated and shown in Supp. Fig. S6A and B. For both metabolites, there are no significant differences in the specific uptake rates. Thus, every single cell has the same metabolic rate for glucose and glutamine. In literature, some studies did not see any effect on key metabolites at different levels of hydromechanical stress [15,16,28] whereas Keane et al. even observed an increasing glucose uptake with higher hydromechanical stress [53].

Summing up, the data provide a detailed insight into the culture behavior and key metabolites of CHO DP12 cells at different  $\varepsilon_0$  leading to new findings concerning sub-lethal effects caused by hydromechanical stress. However, the lactate concentration was not considered yet. The lactate switch, which is a common phenomenon for CHO cells [54], will be analyzed by the offline data shown in Fig. 4.

The offline lactate concentrations are shown in Fig. 4A. They point out that the time at which the lactate is depleted completely – before it starts rising again – is shifted with increasing  $\varepsilon_0$ . The shift is so clear so that it is well seen from offline data even though they were sampled only once a day. For all  $\varepsilon_0$ , the lactate concentrations rise for the first 3–4 cultivation days. For the three lowest  $\varepsilon_0$  the lactate concentrations decrease rapidly afterward while the concentrations for the two highest  $\varepsilon_0$  stay high for about three days before they drop again. In Fig. 4B, the time points at which lactate dropped to zero were set in relation to the standard cultivation with  $\varepsilon_0 = 0.12 \text{ W kg}^{-1}$  and plotted against  $\varepsilon_0$  in a semi-logarithmic plot. The plot quantifies the lactate switch. As becomes evident, the time of lactate switch is correlated to the logarithm of  $\varepsilon_0$  similarly to glucose and glutamine depletion. In addition, the cell-specific lactate production rate was calculated and plotted in Supp. Fig. S6C. In accordance with the results of specific glucose and glutamine uptake, there are in overall no significant differences in the cell-specific lactate uptake rates.

When looking at the results as a whole, it can be said that the whole cells grow more slowly with increased  $\varepsilon_0$  and thus show delayed consumption of key metabolites. As mentioned before, this can be due to two reasons: 1. each individual cell doubles more slowly or 2. not all cells survive under increased hydromechanical stress. The first theory is in contrast to the calculated cell-specific uptake and production rates, as these do not differ significantly for varying  $\varepsilon_0$ . However, the second theory is in contrast to Kolmogorov's length of microscale. According to this theory, the cells should only be destroyed by the eddies at the highest  $\varepsilon_0$ . However, both approaches have weaknesses. The determination of the cell-specific uptake and production rates is very imprecise, as on the one hand the individual measurement results are subject to errors (the errors are particularly high for glutamine concentrations) and on the other hand the data density is low. Considerably higher sample densities would be necessary to make more accurate statements.

Kolmogorov's length of microscale is an old, empirically theory which provides guide values for the size of the eddies. Therefore, the reason for slowed respiratory activity cannot be answered completely.

Summarizing the effects of varying hydromechanical stress on CHO DP12's metabolism, an increasing  $\varepsilon_0$  leads to a delayed depletion of nutrients: the time for glucose and glutamine depletion and the lactate switch increase with logarithmically increasing  $\varepsilon_0$  while  $\mu_{\max}$  decreases. The cell-specific uptake and production rates do not differ significantly. The key metabolites are important parameters for a successful CHO cultivation process, but productivity is the most essential parameter. Therefore, the analysis of the antibody production follows.

#### 3.4. Influence of varying $\varepsilon_0$ on the antibody production

The CHO DP12 cell line produces an IgG antibody. Its concentration was measured by Protein A chromatography over the whole cultivation process for all experiments (see Supp. Fig. S7). To compare the final antibody titers, the last three measured values were averaged and plotted against the logarithm of  $\varepsilon_0$ . The results are depicted in Fig. 5.

As becomes obvious from Fig. 5., the antibody concentration is similar within the standard deviations for all experiments up to  $\varepsilon_0 = 1.45 \text{ W kg}^{-1}$  and reaches the reported maximal product titer for this cell line of roughly  $250 \text{ mg L}^{-1}$ . In contrast, the final antibody concentration for the cultivation with the highest  $\varepsilon_0$  ( $3.84 \text{ W kg}^{-1}$ ) was only approximately  $180 \text{ mg L}^{-1}$  (orange left side triangle) and is statistically different to the other concentrations ( $p < 0.001$ ). To explain this difference, it is important to consider  $\varepsilon_{\max}$ . The consideration is irrelevant in shake flasks if the Reynolds number is  $< 60,000$ . Under these conditions, there is a laminar flow in the shake flask and  $\varepsilon_{\max}$  is equal to  $\varepsilon_0$  [45]. This applies to all cultivations except for the one with the highest  $\varepsilon_0$  (see Table 1). For the latter, a Re of 76 508 was calculated according to Eq. (3). That means under these conditions the flow should be turbulent.  $\varepsilon_{\max}$  was calculated according to Eq. (4) and is approximately  $17 \text{ W kg}^{-1}$ . Thus, it is about four times greater than  $\varepsilon_0$ . Therefore, the hydromechanical forces in this cultivation were much higher than in all the other ones and, the flow regime was different. Nienow already stated that the flow regime is an important factor for the influence of hydro-mechanical stress on mammalian cells [7] and Neunstöcklin et al. found that CHO cells were more sensitive at turbulent flow conditions than at laminar flows [5]. According to Kolmogorov's theory, the cells should be influenced by the eddies which could also have an influence on antibody production. In general, low growth rates of CHO cells are associated with higher productivity independently from different  $\varepsilon$  [55]. Different growth rates caused by increasing  $\varepsilon$  did not lead to higher final antibody concentrations in this study. Additionally, the cell-specific antibody productivity (see Supp. Fig. S6D) is not statistically different for any of the cultivations.

To sum up, the final antibody titer is not influenced by varying energy dissipation in the laminar flow regime, but if a turbulent regime is present, the final titer declined about 40 %. For future investigations of hydromechanical stress and antibody production, the analysis of antibody activity and glycosylation profiles would be of high interest.

## 4. Conclusion

This study examined the influence of varying levels of hydromechanical stress on CHO DP12 shake flask cultivations. The energy dissipation was used as a quantifiable variable that describes the hydromechanical stress. The cultivation under standard conditions ( $\varepsilon_0 = 0.12 \text{ W kg}^{-1}$ ) showed that the OTR is a suitable parameter to evaluate the metabolism – especially glucose and glutamine depletion – of a CHO DP12 cell culture. By varying  $\varepsilon_0$ , it could be demonstrated that an increase in the hydromechanical stress leads to a slowdown in the respiration activity and prolongs the cultivation process. The tested  $\varepsilon_0$  range was in the largest feasible range for shake flask cultures which are limited due to the technical specifications of standard shakers. Under



these conditions, they cannot be operated at higher shaking speeds than 450 rpm. No lethal effects were noticed in the entire range. A halt in cell growth was also not observed. The viable maximal cell density decreased with increasing  $\varepsilon_0$ . A detailed examination of the respiratory activity showed that  $\mu_{\max}$ , the time for glucose and glutamine depletion, and the lactate switch correlate linear with logarithmically plotted  $\varepsilon_0$ . Cell-specific uptake and production rates did not statistically differ between the cultivations. The antibody titer reaches the highest reported value for this cell line ( $250 \text{ mg L}^{-1}$ ) for all cultivations within a laminar flow. In the only cultivation within a turbulent flow ( $\varepsilon_0 = 3.84 \text{ W kg}^{-1}$ ), the final titer was reduced by about 40 %.

This study showed that the influence of hydromechanical stress on CHO cells in shake flasks can be easily analyzed. As shake flasks are easy to handle and cost-efficient, this is a simple method to examine the influence on other, possibly more sensitive cells. Hydromechanical stress is a key parameter for the scale-up of mammalian cell culture processes. Therefore, the findings from this study should provide a good basis for a data-driven scale-up of animal cells from shake flasks to STRs.

### CRedit authorship contribution statement

**Anne Neuss:** Writing – review & editing, Writing – original draft, Visualization, Methodology, Investigation, Formal analysis, Data curation, Conceptualization. **Jacinta Sofia Tomas Borges:** Methodology, Investigation. **Nele von Vegesack:** Methodology, Investigation. **Jochen Büchs:** Writing – review & editing, Supervision. **Jorgen Barsett Magnus:** Writing – review & editing, Supervision, Resources.

### Declaration of Competing Interest

The authors declare that they have no known competing financial interests or personal relationships that could have appeared to influence the work reported in this paper.

### Data Availability

Data will be made available on request.

### Acknowledgments

We thank Thomas Noll (Bielefeld University) for providing the CHODP12 cell line and 4BioCell for providing the automated cell counter (CEDEX). Special thanks to Heino Büntemeyer (Bielefeld University) for help with the Protein A method. We thank Eva Forsten (RWTH Aachen University) for providing the MATLAB® script for  $\mu_{\max}$  calculations.

### Appendix A. Supporting information

Supplementary data associated with this article can be found in the online version at [doi:10.1016/j.nbt.2024.09.008](https://doi.org/10.1016/j.nbt.2024.09.008).

### References

- Sharker SM, Rahman A. A review on the current methods of Chinese hamster ovary (CHO) cells cultivation for the production of therapeutic protein. *Curr Drug Discov Technol* 2021;18(3):354–64. <https://doi.org/10.2174/1570163817666200312102137>.
- Walsh G, Walsh E. Biopharmaceutical benchmarks 2022. *Nat Biotechnol* 2022;40(12):1722–60. <https://doi.org/10.1038/s41587-022-01582-x>.
- Zhang J-H, Shan L-L, Liang F, Du C-Y, Li J-J. Strategies and considerations for improving recombinant antibody production and quality in Chinese hamster ovary cells. *Front Bioeng Biotechnol* 2022;10:856049. <https://doi.org/10.3389/fbioe.2022.856049>.
- Nagashima H, Watari A, Shinoda Y, Okamoto H, Takuma S. Application of a quality by design approach to the cell culture process of monoclonal antibody production, resulting in the establishment of a design space. *J Pharm Sci* 2013;102(12):4274–83. <https://doi.org/10.1002/jps.23744>.
- Neunstoecklin B, Stettler M, Solacroup T, Broly H, Morbidelli M, Soos M. Determination of the maximum operating range of hydrodynamic stress in mammalian cell culture. *J Biotechnol* 2015;194:100–9. <https://doi.org/10.1016/j.jbiotec.2014.12.003>.
- Chalmers JJ. Mixing, aeration and cell damage, 30+ years later: what we learned, how it affected the cell culture industry and what we would like to know more about. *Curr Opin Chem Eng* 2015;10:94–102. <https://doi.org/10.1016/j.coche.2015.09.005>.
- Nienow AW, Scott WH, Hewitt CJ, Thomas CR, Lewis G, Amanullah A, et al. Scale-down studies for assessing the impact of different stress parameters on growth and product quality during animal cell culture. *Chem Eng Res Des* 2013;91(11):2265–74. <https://doi.org/10.1016/j.cherd.2013.04.002>.
- Hu W, Berdugo C, Chalmers JJ. The potential of hydrodynamic damage to animal cells of industrial relevance: current understanding. *Cytotechnology* 2011;63(5):445–60. <https://doi.org/10.1007/s10616-011-9368-3>.
- Chalmers JJ, Ma N. Hydrodynamic damage to animal cells. *Animal Cell Culture*. 2015th ed. Cham: Springer International Publishing; 2015. p. 169–83.
- Al-Rubeai M, Singh RP, Goldman MH, Emery AN. Death mechanisms of animal cells in conditions of intensive agitation. *Biotech Bioeng* 1995;45(6):463–72. <https://doi.org/10.1002/bit.260450602>.
- Kunas KT, Papoutsakis ET. Damage mechanisms of suspended animal cells in agitated bioreactors with and without bubble entrainment. *Biotech Bioeng* 1990;36(5):476–83. <https://doi.org/10.1002/bit.260360507>.
- Oh S, Nienow AW, Al-Rubeai M, Emery AN. The effects of agitation intensity with and without continuous sparging on the growth and antibody production of hybridoma cells. *J Biotechnol* 1989;12(1):45–61. [https://doi.org/10.1016/0168-1656\(89\)90128-4](https://doi.org/10.1016/0168-1656(89)90128-4).
- Paul K, Herwig C. Scale-down simulators for mammalian cell culture as tools to access the impact of inhomogeneities occurring in large-scale bioreactors. *Eng Life Sci* 2020;20(5-6):197–204. <https://doi.org/10.1002/elsc.201900162>.
- Daub A, Böhm M, Delueg S, Mühlmann M, Schneider G, Büchs J. Characterization of hydromechanical stress in aerated stirred tanks up to 40 m(3) scale by measurement of maximum stable drop size. *J Biol Eng* 2014;8(1):17. <https://doi.org/10.1186/1754-1611-8-17>.
- Sieck JB, Cordes T, Budach WE, Rhiel MH, Suemeghy Z, Leist C, et al. Development of a scale-down model of hydrodynamic stress to study the performance of an industrial CHO cell line under simulated production scale bioreactor conditions. *J Biotechnol* 2013;164(1):41–9. <https://doi.org/10.1016/j.jbiotec.2012.11.012>.
- Sieck JB, Budach WE, Suemeghy Z, Leist C, Villiger TK, Morbidelli M, et al. Adaptation for survival: phenotype and transcriptome response of CHO cells to elevated stress induced by agitation and sparging. *J Biotechnol* 2014;189:94–103. <https://doi.org/10.1016/j.jbiotec.2014.08.042>.
- Maschke RW, Seidel S, Bley T, Eibl R, Eibl D. Determination of culture design spaces in shaken disposable cultivation systems for CHO suspension cell cultures. *Biochem Eng J* 2022;177:108224. <https://doi.org/10.1016/j.bej.2021.108224>.
- Hunt JCR, Vassilicos JC. Kolmogorov's contributions to the physical and geometrical understanding of small-scale turbulence and recent developments. *Proc R Soc Lond A* 1991;434(1890):183–210. <https://doi.org/10.1098/rspa.1991.0088>.
- Nienow AW. Scale-up considerations based on studies at the bench scale in stirred bioreactors. *J Chem Eng Jpn* 2009;42(11):789–96. <https://doi.org/10.1252/jcej.08we317>.
- Nienow AW. Reactor engineering in large scale animal cell culture. *Cytotechnology* 2006;50(1-3):9–33. <https://doi.org/10.1007/s10616-006-9005-8>.
- Henzi H-J, Biedermann A. Modelluntersuchungen zur partikelbeanspruchung in reaktoren. *Chem Ing Tech* 1996;68(12):1546–61. <https://doi.org/10.1002/cite.330681205>.
- Peter CP, Suzuki Y, Büchs J. Hydromechanical stress in shake flasks: correlation for the maximum local energy dissipation rate. *Biotech Bioeng* 2006;93(6):1164–76. <https://doi.org/10.1002/bit.20827>.
- Panckow RP, Bliatsiou C, Nolte L, Böhm L, Maaß S, Kraume M. Characterisation of particle stress in turbulent impeller flows utilising photo-optical measurements of a flocculation system – PART 1. *Chem Eng Sci* 2023;267:118333. <https://doi.org/10.1016/j.ces.2022.118333>.
- Villiger TK, Morbidelli M, Soos M. Experimental determination of maximum effective hydrodynamic stress in multiphase flow using shear sensitive aggregates. *AIChE J* 2015;61(5):1735–44. <https://doi.org/10.1002/aic.14753>.
- Ma N, Koelling KW, Chalmers JJ. Fabrication and use of a transient contractional flow device to quantify the sensitivity of mammalian and insect cells to hydrodynamic forces. *Biotech Bioeng* 2002;80(4):428–37. <https://doi.org/10.1002/bit.10387>.
- Mollet M, Ma N, Zhao Y, Brodkey R, Taticek R, Chalmers JJ. Bioprocess equipment: characterization of energy dissipation rate and its potential to damage cells. *Biotechnol Prog* 2004;20(5):1437–48. <https://doi.org/10.1021/bp0498488>.
- Godoy-Silva R, Chalmers JJ, Casnocha SA, Bass LA, Ma N. Physiological responses of CHO cells to repetitive hydrodynamic stress. *Biotech Bioeng* 2009;103(6):1103–17. <https://doi.org/10.1002/bit.22339>.
- Godoy-Silva R, Mollet M, Chalmers JJ. Evaluation of the effect of chronic hydrodynamical stresses on cultures of suspended CHO-6E6 cells. *Biotech Bioeng* 2009;102(4):1119–30. <https://doi.org/10.1002/bit.22146>.
- Neunstoecklin B, Villiger TK, Lucas E, Stettler M, Broly H, Morbidelli M, et al. Pilot-scale verification of maximum tolerable hydrodynamic stress for mammalian cell culture. *Appl Microbiol Biotechnol* 2016;100(8):3489–98. <https://doi.org/10.1007/s00253-015-7193-x>.



- [30] Hernández Rodríguez T, Pörtner R, Frahm B. Seed train optimization for suspension cell culture. *BMC Proc* 2013;7(S6). <https://doi.org/10.1186/1753-6561-7-S6-P9>.
- [31] Zhang X, Stettler M, Sanctis D de, Perrone M, Parolini N, Discacciati M, et al. Use of orbital shaken disposable bioreactors for mammalian cell cultures from the milliliter-scale to the 1,000-liter scale. *Adv Biochem Eng Biotechnol* 2009;115:33–53. [https://doi.org/10.1007/10\\_2008\\_18](https://doi.org/10.1007/10_2008_18).
- [32] Büchs J, Zoels B. Evaluation of maximum to specific power consumption ratio in shaking bioreactors. *J Chem Eng Jpn / JCEJ* 2001;34(5):647–53. <https://doi.org/10.1252/jcej.34.647>.
- [33] Pérez-Rodríguez S, Reynoso-Cereceda GI, Valdez-Cruz NA, Trujillo-Roldán MA. A comprehensive comparison of mixing and mass transfer in shake flasks and their relationship with MAb productivity of CHO cells. *Bioprocess Biosyst Eng* 2022;45(6):1033–45. <https://doi.org/10.1007/s00449-022-02722-y>.
- [34] Gaugler L, Hofmann S, Schlüter M, Takors R. Mimicking CHO large-scale effects in the single multicompartment bioreactor: a new approach to access scale-up behavior. *Biotech Bioeng* 2024;121(4):1244–56. <https://doi.org/10.1002/bit.28647>.
- [35] Ihling N, Munkler LP, Berg C, Reichenbächer B, Wirth J, Lang D, et al. Time-resolved monitoring of the oxygen transfer rate of Chinese Hamster Ovary cells provides insights into culture behavior in shake flasks. *Front Bioeng Biotechnol* 2021;9:725498. <https://doi.org/10.3389/fbioe.2021.725498>.
- [36] Ihling N, Munkler LP, Paul R, Berg C, Reichenbächer B, Kadisch M, et al. Non-invasive and time-resolved measurement of the respiration activity of Chinese hamster ovary cells enables prediction of key culture parameters in shake flasks. *Biotechnol J* 2022;17(8):e2100677. <https://doi.org/10.1002/biot.202100677>.
- [37] Stöckmann C, Maier U, Anderlei T, Knocke C, Gellissen G, Büchs J. The oxygen transfer rate as key parameter for the characterization of *Hansenula polymorpha* screening cultures. *J Ind Microbiol Biotechnol* 2003;30(10):613–22. <https://doi.org/10.1007/s10295-003-0090-9>.
- [38] Martínez-Monge I, Roman R, Comas P, Fontova A, Lecina M, Casablanca A, et al. New developments in online OUR monitoring and its application to animal cell cultures. *Appl Microbiol Biotechnol* 2019;103(17):6903–17. <https://doi.org/10.1007/s00253-019-09989-4>.
- [39] Maschke RW, John GT, Eibl D. Monitoring of oxygen, pH, CO<sub>2</sub> and biomass in smart single-use shake flasks. *Chem Ing Tech* 2022;94(12):1995–2001. <https://doi.org/10.1002/cite.202200094>.
- [40] Ihling N, Munkler LP, Paul R, Lang D, Büchs J. Introducing oxygen transfer rate measurements as a novel method for time-resolved cytotoxicity assessment in shake flasks. *Environ Sci Eur* 2022;34(1):1–15. <https://doi.org/10.1186/s12302-022-00673-5>.
- [41] Neuss A, Vegesack N, von, Liepelt R, Büchs J, Barsett Magnus J. Online monitoring of the respiration activity in 96-deep-well microtiter plate Chinese hamster ovary cultures streamlines kill curve experiments. *Biotechnol Prog* 2024:e3468. <https://doi.org/10.1002/btpr.3468>.
- [42] Anderlei T, Büchs J. Device for sterile online measurement of the oxygen transfer rate in shaking flasks. *Biochem Eng J* 2001;7(2):157–62. [https://doi.org/10.1016/S1369-703X\(00\)00116-9](https://doi.org/10.1016/S1369-703X(00)00116-9).
- [43] Anderlei T, Zang W, Papaspyrou M, Büchs J. Online respiration activity measurement (OTR, CTR, RQ) in shake flasks. *Biochem Eng J* 2004;17(3):187–94. [https://doi.org/10.1016/S1369-703X\(03\)00181-5](https://doi.org/10.1016/S1369-703X(03)00181-5).
- [44] Büchs J, Maier U, Milbradt C, Zoels B. Power consumption in shaking flasks on rotary shaking machines: I. Power consumption measurement in unbaffled flasks at low liquid viscosity. *Biotech Bioeng* 2000;68(6):589–93. [https://doi.org/10.1002/\(SICI\)1097-0290\(20000620\)68:6<589:AID-BIT1>3.0.CO;2-J](https://doi.org/10.1002/(SICI)1097-0290(20000620)68:6<589:AID-BIT1>3.0.CO;2-J).
- [45] Klöckner W, Büchs J. Advances in shaking technologies. *Trends Biotechnol* 2012;30(6):307–14. <https://doi.org/10.1016/j.tibtech.2012.03.001>.
- [46] Forsten, Eva, Gerdes, Steffen, Petri, René, Büchs, Jochen and Magnus, Jorgen. Unraveling the impact of pH, sodium concentration, and medium osmolality on *Vibrio natriegens* in batch processes. *BMC Biotechnol*. <https://doi.org/10.1186/s12896-024-00897-8>.
- [47] Hansen S, Hariskos I, Luchterhand B, Büchs J. Development of a modified respiration activity monitoring system for accurate and highly resolved measurement of respiration activity in shake flask fermentations. *J Biol Eng* 2012;6(1):11. <https://doi.org/10.1186/1754-1611-6-11>.
- [48] Kottmeier K, Müller C, Huber R, Büchs J. Increased product formation induced by a directed secondary substrate limitation in a batch *Hansenula polymorpha* culture. *Appl Microbiol Biotechnol* 2010;86(1):93–101. <https://doi.org/10.1007/s00253-009-2285-0>.
- [49] Sparviero S, Dicke MD, Rosch TM, Castillo T, Salgado-Lugo H, Galindo E, et al. Yeast extracts from different manufacturers and supplementation of amino acids and micro elements reveal a remarkable impact on alginate production by *A. vinelandii* ATCC9046. *Micro Cell Fact* 2023;22(1):99. <https://doi.org/10.1186/s12934-023-02112-3>.
- [50] Strasser L, Farrell A, Ho JTC, Scheffler K, Cook K, Pankert P, et al. Proteomic profiling of IgG1 producing CHO cells using LC/LC-SPS-MS3: the effects of bioprocessing conditions on productivity and product quality. *Front Bioeng Biotechnol* 2021;9:569045. <https://doi.org/10.3389/fbioe.2021.569045>.
- [51] Klausung S, Krämer O, Noll T. Enhancing cell growth and antibody production in CHO cells by siRNA knockdown of novel target genes. *BMC Proc* 2013;7(S6). <https://doi.org/10.1186/1753-6561-7-S6-P92>.
- [52] Tanzglock T, Soos M, Stephanopoulos G, Morbidelli M. Induction of mammalian cell death by simple shear and extensional flows. *Biotech Bioeng* 2009;104(2):360–70. <https://doi.org/10.1002/bit.22405>.
- [53] Keane JT, Ryan D, Gray PP. Effect of shear stress on expression of a recombinant protein by Chinese hamster ovary cells. *Biotech Bioeng* 2003;81(2):211–20. <https://doi.org/10.1002/bit.10472>.
- [54] Zagari F, Jordan M, Stettler M, Broly H, Wurm FM. Lactate metabolism shift in CHO cell culture: the role of mitochondrial oxidative activity. *N Biotechnol* 2013;30(2):238–45. <https://doi.org/10.1016/j.nbt.2012.05.021>.
- [55] Kim DY, Chaudhry MA, Kennard ML, Jardon MA, Braasch K, Dionne B, et al. Fed-batch CHO cell t-PA production and feed glutamine replacement to reduce ammonia production. *Biotechnol Prog* 2013;29(1):165–75. <https://doi.org/10.1002/btpr.1658>.